[redacted]

Copy 228
RM L56F21

Reg # 12739

TECH LIBRARY KAFB, NM
0144210

NACA RM L56F21

7706

NACA

RESEARCH MEMORANDUM

TRANSONIC WIND-TUNNEL INVESTIGATION OF STATIC LONGITUDINAL FORCE AND MOMENT CHARACTERISTICS OF TWO WING-BODY COMBINATIONS WITH CLIPPED-TIP AND FULL DELTA WINGS OF ASPECT RATIO 1.73

By Dale L. Burrows

Langley Aeronautical Laboratory
Langley Field, Va.

[redacted]

[redacted] Title 18, U.S.C., Secs. 793 and 794, the transmission or revelation of which in [redacted] manner to an unauthorized person [redacted] by law.

NATIONAL ADVISORY COMMITTEE
FOR AERONAUTICS
WASHINGTON
September 14, 1956

[redacted]

TECH LIBRARY KAFB, NM

0144210

NATIONAL ADVISORY COMMITTEE FOR AERONAUTICS

RESEARCH MEMORANDUM

TRANSONIC WIND-TUNNEL INVESTIGATION OF STATIC LONGITUDINAL FORCE AND MOMENT CHARACTERISTICS OF TWO WING-BODY COMBINATIONS WITH CLIPPED-TIP AND FULL DELTA WINGS OF ASPECT RATIO 1.73

By Dale L. Burrows

SUMMARY

An investigation has been made in the Langley transonic blowdown tunnel to obtain the static longitudinal force and moment characteristics of an aspect-ratio-1.73, 3-percent-thick delta wing and an aspect-ratio-1.73, 4-percent-thick clipped delta wing (taper ratio 0.4), each mounted on a slender body. Both wings had NACA 65A00X airfoil sections parallel to the body center line. The Mach number range was from 0.76 to 1.39 at angles of attack as high as 20°. At low angles of attack, the Reynolds number was about 7×10^6 for the full delta and 6×10^6 for the clipped delta.

Results of the investigation indicate that although the clipped wing had a 9- to 15-percent higher lift-curve slope throughout the Mach number range, the full delta had appreciably lower zero-lift drags, 6- to 20-percent higher lift-drag ratios, and a much smaller shift in aerodynamic center with change in Mach number.

INTRODUCTION

The advance of airplane operational speeds into and through the transonic range has led to an increased need for aerodynamic information on low-aspect-ratio wings. The combined considerations of low drag, satisfactory stability, and airframe strength have led to compromises in leading-edge sweep, wing thickness, and aspect ratio. Several investigations have provided information on the longitudinal characteristics of thin, swept, low-aspect-ratio wings. For example, in reference 1 the high subsonic and low supersonic characteristics have been summarized for a rather large number of wing-fuselage configurations

employing low-aspect-ratio wings of various plan forms; the Reynolds numbers for these tests ranged from about 2.5×10^6 to about 7×10^6. For the transonic speed range, references 2 and 3 present rather small-scale results of extensive systematic investigations of the wing-alone characteristics of thin, low-aspect-ratio, tapered wings by the transonic-bump technique. To provide transonic information on wing-body configurations at relatively large scale, a series of investigations was made in the Langley transonic blowdown tunnel. The first three investigations of the series have been reported in references 4, 5, and 6. The present report contains the characteristics of two aspect-ratio-1.73 wings, one of full delta plan form and 3-percent thickness and the other of clipped delta plan form (taper ratio 0.4) and 4-percent thickness. The differences in thickness were chosen to provide approximate structural equivalence on the basis of root bending stresses. The tests were made with the wings mounted on a slender body at Mach numbers from 0.76 to 1.39 at angles of attack up to 20°. The Reynolds number based on the mean aerodynamic chord was about 6.5×10^6 at angles of attack up to 12° and about 3.2×10^6 at angles of attack from 10° to 20°.

SYMBOLS

C_D	drag coefficient, Drag/qS
C_{D_0}	drag coefficient at zero lift
ΔC_D	increment of drag at optimum lift, $C_D \left(\text{at } C_{L_{opt}}\right) - C_{D_0}$
C_L	lift coefficient, Lift/qS
C_m	pitching-moment coefficient, $\dfrac{\text{Pitching moment about } \bar{c}/4}{qS\bar{c}}$
L/D	lift-drag ratio
$(L/D)_{max}$	maximum value of lift-drag ratio
$C_{L_{opt}}$	lift coefficient at $(L/D)_{max}$
A	aspect ratio
b	total wing span

c	wing chord at any value of y
$\bar{c}$	wing mean aerodynamic chord, $\frac{2}{S}\int_0^{b/2} c^2 dy$
M	free-stream Mach number at model location
p	free-stream static pressure
p_t	free-stream absolute stagnation pressure
q	free-stream dynamic pressure, $\gamma p M^2/2$
R	free-stream Reynolds number based on $\bar{c}$
S	total wing area
y	spanwise distance from model center line
α	angle of attack of model center line, deg
γ	ratio of specific heats, 1.4 for air
λ	taper ratio, $\frac{\text{Tip chord}}{\text{Root chord}}$

APPARATUS AND METHODS

Models

Geometric details of the two wing-body configurations are shown in figure 1. Both wings had an aspect ratio of 1.73 and NACA 65A00X airfoil sections parallel to the model center line and were located on the body so that the $\bar{c}/4$ point for each wing was at the same longitudinal body station. The full delta wing had a 67° leading-edge sweep and 3-percent thickness. The clipped delta wing had a 45° leading-edge sweep and 4-percent thickness.

The tip of the latter wing (hereafter referred to as the clipped wing) was formed by revolution of the tip-section ordinates about the chord line. All wings were solid steel and were mounted with zero incidence and zero dihedral at the body center line.

The body was a hollow steel shell having an ogival nose 3.5 diameters in length and a cylindrical afterbody. The fineness ratio of the body was 9.63. The radius of curvature of the ogival nose was 12.5 body diameters.

Tunnel

The investigation was conducted in the Langley transonic blowdown tunnel in which Mach numbers up to 1.4 can be attained. At a given Mach number, the Reynolds number can be varied from approximately 8×10^6 to 24×10^6 per foot of chord by varying the stagnation pressure from 25 to 70 lb/sq in. abs. (psia). Mach number distribution at the model location was constant within ± 0.01. (See ref. 4 for distribution.)

Tests

The investigation covered a Mach number range from 0.67 to 1.30 at angles of attack from about 0° to 12° for a stagnation pressure of 70 lb/sq in. abs and at angles of attack from 10° to 20° for a stagnation pressure of 35 lb/sq in. abs. For a Mach number of 1.38, data were obtained at a stagnation pressure of 50 lb/sq in. abs at angles of attack from about 0° to 12°. The limits of angle of attack were dictated by balance load limitations or by the angle-of-attack mechanism. Reynolds numbers based on $\bar{c}$ for the various stagnation pressures are shown in figure 2. For all tests, the surface of the model was in a smooth condition. Shock reflections from the tunnel wall intersected the model at Mach numbers between about 1.04 and 1.10. Inasmuch as this condition introduces tunnel-wall effects on the force and moment data which may be appreciable, no data are presented in this Mach number range.

Measurements

The model was attached to an internal three-component strain-gage balance which in turn was attached to a sting support. (See fig. 1.) Two small pressure tubes extended inside the base of the body for the purpose of recording base pressures. Normal force, chord force, pitching moment, and base-pressure data were recorded simultaneously on film. The chord-force coefficient was adjusted to a condition of base pressure equal to free-stream static pressure. Normal- and chord-force coefficients were converted to lift and drag coefficients by the usual methods. In addition to the previously mentioned error in Mach number distribution, there is a variation of Mach number with angle of attack, and the overall accuracy is within ± 0.015.

Corrections

Reference 7 shows that for slotted tunnels where the ratio of model size to tunnel size is about that of the present investigation, the subsonic jet-boundary effects are negligible; therefore, no such correction has been made to the data. Angle of attack was corrected for sting and balance deflection resulting from aerodynamic load.

In reference 4, bench tests were reported for an aspect-ratio-3, 3-percent-thick delta wing to estimate the aeroelastic effects. For that case, it was found that for the largest forces measured aeroelasticity produced a 2-percent decrease in lift-curve slope and less than $0.01\bar{c}$ forward shift in aerodynamic center. It would be expected that for the present lower aspect ratio (1.73), the aeroelastic effects would be even less. In the data presented, therefore, no correction for aeroelasticity has been applied. No other systematic errors are known to exist and, in regard to random errors, it is believed that an indication of the accuracy of the data can best be determined from the scatter of test points.

PRESENTATION OF RESULTS

The results of the investigation are presented as follows:

	Figure
C_L against α for -	
Full delta wing	3(a)
Clipped delta wing	3(b)
$\left(dC_L/d\alpha\right)_{C_L=0}$ against M for both wings	4
C_D against C_L for -	
Full delta wing	5(a)
Clipped delta wing	5(b)
C_D (at C_L = 0, 0.1, 0.2, 0.3, 0.4, and 0.5) against M for both wings	6
Longitudinal area development	7
L/D against C_L for both wings	8

Figure

$(L/D)_{max}$ and $C_{L_{opt}}$ against Mach number for both wings 9

Drag-due-to-lift factor against M at $C_{L_{opt}}$ 10

C_L against C_m for -
Full delta wing . . . . . 11(a)
Clipped delta wing . . . . . 11(b)

$\left(dC_m/dC_L\right)_{C_L=0}$ against M for both wings 12

DISCUSSION

Lift Characteristics

The basic data of lift coefficient against angle of attack are presented in figure 3. The lift curves for both wings are linear through the Mach number range up to values of the lift coefficient of about 0.3 for the full delta wing and 0.2 for the clipped delta wing. At higher lift coefficients, the lift-curve slope for the clipped delta wing was markedly more nonlinear throughout the Mach number range than was that for the full delta. Similar degrees of nonlinearity in low-aspect-ratio lift-curve slopes were presented in reference 8 for a full delta and a clipped delta wing. The greater increase in lift-curve slope at moderate lifts for the clipped wing indicates that the increase in lift due to swept-leading-edge vortex formation more than outweighs the decrease in lift that may occur as a result of separated flow over the tip. These two effects on lift are more nearly balanced for the full delta wing, as indicated by the nearly linear variation of lift with angle of attack through the moderate lift range. The extension of the nonlinearity into the supersonic range indicates that the wing responds largely to subsonic flow phenomena. Although maximum lift was not attained on either wing, the rounding off of the lift curve for the clipped wing at the higher angles of attack and through the subsonic Mach number range suggests a somewhat lower maximum lift for the clipped wing than for the full delta wing. This would be expected on the basis of greater leading-edge vortex strength for the wing with highest sweep. (See ref. 9.)

A plot of lift-curve slope presented in figure 4 for the two wings indicates that at zero lift the clipped wing has about 9 percent more lifting efficiency than the full delta wing in the subsonic range and about 15 percent more in the supersonic range. Although this result is

largely due to differences in leading-edge sweep, some of the difference in lift-curve slope is partly due to the fact that the exposed area of the clipped wing is larger and partly due to the fact that separation may begin to occur on the tips of the full delta wing at very low angles of attack. It would not be expected that the difference in thickness of the two wings would contribute measureably to their differences in lift variation at the low angles of attack. (See, for example, the negligible differences due to thickness discussed in reference 5.)

The method of reference 10 has been used to determine the theoretical lift-curve slopes of the wing-body combinations. This method required wing-alone lift-curve slopes which were obtained from the theories of DeYoung (ref. 11) and Lapin (ref. 12), respectively, for the subsonic and supersonic speed ranges. Although theoretical potential-flow lift-curve slopes are usually greater than experimental slopes, the theoretical values calculated for the present wings of aspect ratio 1.73 were generally less than or equal to the measured values. Even though in reference 5, the method predicted as expected for aspect ratios of 3 and above, the present theoretical result, for subsonic Mach numbers at least, seems to indicate an inadequacy of the theory for aspect ratios as low as 1.73. A better indication of lift-curve slope for the low-aspect-ratio wings in the high subsonic Mach number range may be obtained by the methods of reference 13.

Drag Characteristics

Basic drag data in coefficient form are plotted against lift coefficient in figures 5(a) and 5(b). A cross plot of drag against Mach number at constant lift in figure 6 indicates that at zero lift the clipped wing has an appreciably higher drag coefficient than the full delta wing throughout the Mach number range; this was probably largely due to differences in exposed surface area and to a lesser extent due to differences in Reynolds number. The zero-lift transonic drag rise was more abrupt and the supersonic drag was higher for the clipped wing because of less sweep, greater wing thickness ratio, larger exposed wing area, and a less favorable area distribution. (See fig. 7.) As the lift coefficient was increased, relationship between the drag curves for the wings reversed from that at zero lift; at the higher lift, the full delta wing had a somewhat higher drag, probably because of the separated flow over the tip.

Values of $(L/D)_{max}$ and $C_{L_{opt}}$ taken from figure 8 are presented in figure 9. The full delta wing had values of $(L/D)_{max}$ from 6 to 20 percent higher than the clipped wing throughout the Mach number range.

These values of $(L/D)_{max}$ occurred at values of the lift coefficient $C_{L_{opt}}$ that were somewhat lower for the full delta than for the clipped wing. Both of the foregoing results are largely due to the differences in zero-lift drag for the two configurations. (See fig. 10 for similarity between the drag-due-to-lift results for the two models.) The general variation in $(L/D)_{max}$ with Mach number for both wings is due about equally to the variation in zero-lift drag and in induced drag, as indicated by a comparison of figure 6 and figure 10.

The calculated values of maximum lift-drag ratio presented in figure 9 were obtained from the relation $\frac{1}{2}\sqrt{\frac{1}{KC_{D_0}}}$. For full leading-edge suction, the induced-drag factor K for subsonic speeds was taken as as $1/\pi A$ and for supersonic speeds the factor was obtained from reference 12; the values of C_{D_0} used were the measured values. In general, it might be expected that the calculated values of $(L/D)_{max}$ for full leading-edge suction would be higher than measured values, especially in the supersonic range. The fact that the theoretical values are lower than the measurements for the clipped wing is an indication of the inadequacy of the method of reference 12 for such low aspect ratios in combination with high taper ratios.

Pitching-Moment Characteristics

The basic pitching-moment curves for the two wings indicate, as shown in figure 11, that the moments for the full delta wing varied linearly with lift throughout the test Mach number range and up to high lifts (except for slight nonlinearity at $M = 0.98$ and 1.01); on the other hand, the moments for the clipped wing varied in a markedly nonlinear manner with lift at the subsonic Mach numbers and gradually became more nearly linear in the supersonic range. Similar differences in the linearity of the pitching-moment curves at subsonic speeds for a clipped and a full delta wing of aspect ratio 2 were presented in reference 1.

The variations of the slope of the pitching-moment curves with Mach number at zero lift are shown in figure 12, where it may be seen that the aerodynamic-center positions for the two wings are widely different, largely because of differences in leading-edge sweep. It is not expected that the differences in thickness of the two wings would contribute measurably to their differences in pitching-moment characteristics. (See, for example, the negligible differences due to thickness discussed in reference 5.) The aerodynamic-center position of the full delta wing had a much smaller and more gradual variation with Mach number than that of the clipped wing.

The theoretical values of aerodynamic center were determined by the method of reference 10. This method required the wing-alone lift-curve slopes, which were obtained from references 11 and 12, and the wing-alone centers of pressure, which were obtained from reference 10. In spite of the inadequacy of the method of references 11 and 12 in predicting lift-curve slopes for low aspect ratios, the theoretical values of aerodynamic-center position are within about $0.06\bar{c}$ of the measured values.

CONCLUSIONS

Tests in the Langley transonic blowdown tunnel to determine the static longitudinal aerodynamic characteristics at transonic speeds of a 4-percent-thick, aspect-ratio-1.73 clipped delta wing and a 3-percent-thick, aspect-ratio-1.73 delta wing, each mounted on a slender body, led to the following conclusions:

1. The clipped wing had a lift-curve slope 9- to 15-percent higher through the test Mach number range of 0.76 to 1.39. The lifts for the clipped wing at high angles of attack suggested a somewhat lower maximum lift than those for the delta wing.

2. The clipped wing had a higher zero-lift drag coefficient throughout the Mach number range than the full delta, mostly because of larger exposed wing area and a smaller chord Reynolds number. Additional factors in the supersonic range were the smaller sweep and greater thickness ratio.

3. The maximum lift-drag ratio for the delta wing was from 6- to 20-percent higher throughout the Mach number range.

4. The aerodynamic center of the full delta wing had a much smaller and a more gradual rearward movement with increases in Mach number than the clipped wing.

Langley Aeronautical Laboratory,
National Advisory Committee for Aeronautics,
Langley Field, Va., June 1, 1956.

REFERENCES

1. Hall, Charles F.: Lift, Drag, and Pitching Moment of Low-Aspect-Ratio Wings at Subsonic and Supersonic Speeds. NACA RM A53A30, 1953.

2. Emerson, Horace F.: Wind-Tunnel Investigation of the Effect of Clipping the Tips of Triangular Wings of Different Thickness, Camber, and Aspect Ratio - Transonic Bump Method. NACA RM A53I03, 1954.

3. Few, Albert G., Jr., and Fournier, Paul G.: Effects of Sweep and Thickness on the Static Longitudinal Aerodynamic Characteristics of a Series of Thin, Low-Aspect-Ratio, Highly Tapered Wings at Transonic Speeds - Transonic-Bump Method. NACA RM L54B25, 1954.

4. Burrows, Dale L., and Palmer, William E.: A Transonic Wind-Tunnel Investigation of the Force and Moment Characteristics of a Plane and a Cambered 3-Percent-Thick Delta Wing of Aspect Ratio 3 on a Slender Body. NACA RM L54H25, 1954.

5. Palmer, William E., and Burrows, Dale L.: A Transonic Wind-Tunnel Investigation of the Longitudinal Force and Moment Characteristics of Two Delta Wings and One Clipped-Tip Delta Wing of 4 Percent Thickness on a Slender Body. NACA RM L55A07a, 1955.

6. Burrows, Dale L., and Tucker, Warren A.: A Transonic Wind-Tunnel Investigation of the Static Longitudinal Characteristics of a 3-Percent-Thick, Aspect-Ratio-3, Delta Wing Cambered and Twisted for High Lift-Drag Ratios. NACA RM L55F02a, 1955.

7. Whitcomb, Charles F., and Osborne, Robert S.: An Experimental Investigation of Boundary Interference on Force and Moment Characteristics of Lifting Models in the Langley 16- and 8-Foot Transonic Tunnels. NACA RM L52L29, 1953.

8. Palmer, William E.: Effect of Reduction in Thickness From 6 to 2 Percent and Removal of the Pointed Tips on the Subsonic Static Longitudinal Stability Characteristics of a 60° Triangular Wing in Combination With a Fuselage. NACA RM L53F24, 1953.

9. Cahill, Jones F., and Gottlieb, Stanley M.: Low-Speed Aerodynamic Characteristics of a Series of Swept Wings Having NACA 65A006 Airfoil Sections (Revised). NACA RM L50F16, 1950.

10. Nielsen, Jack N., Kaattari, George E., and Anastasio, Robert F.: A Method for Calculating the Lift and Center of Pressure of Wing-Body-Tail Combinations at Subsonic, Transonic, and Supersonic Speeds. NACA RM A53G08, 1953.

11. DeYoung, John, and Harper, Charles W.: Theoretical Symmetric Span Loading at Subsonic Speeds for Wings Having Arbitrary Plan Form. NACA Rep. 921, 1948.

12. Lapin, Ellis: Charts for the Computation of Lift and Drag of Finite Wings at Supersonic Speeds. Rep. No. SM-13480, Douglas Aircraft Co., Inc., Oct. 14, 1949.

13. Küchemann, D.: A Non-Linear Lifting-Surface Theory for Wings of Small Aspect Ratio With Edge Separations. Rep. No. Aero. 2540, British R.A.E., Apr. 1955.

Airfoil section parallel to model center line	65A003
Wing area, sq. in.	12.96
Aspect ratio	1.73
Taper ratio	0
Sweepback angle of quarter-chord line	60°
Incidence	0°
Dihedral	0°

Airfoil section parallel to model center line	65A004
Wing area, sq. in.	12.96
Aspect ratio	1.73
Taper ratio	0.4
Sweepback angle of quarter-chord line	37°
Incidence	0°
Dihedral	0°

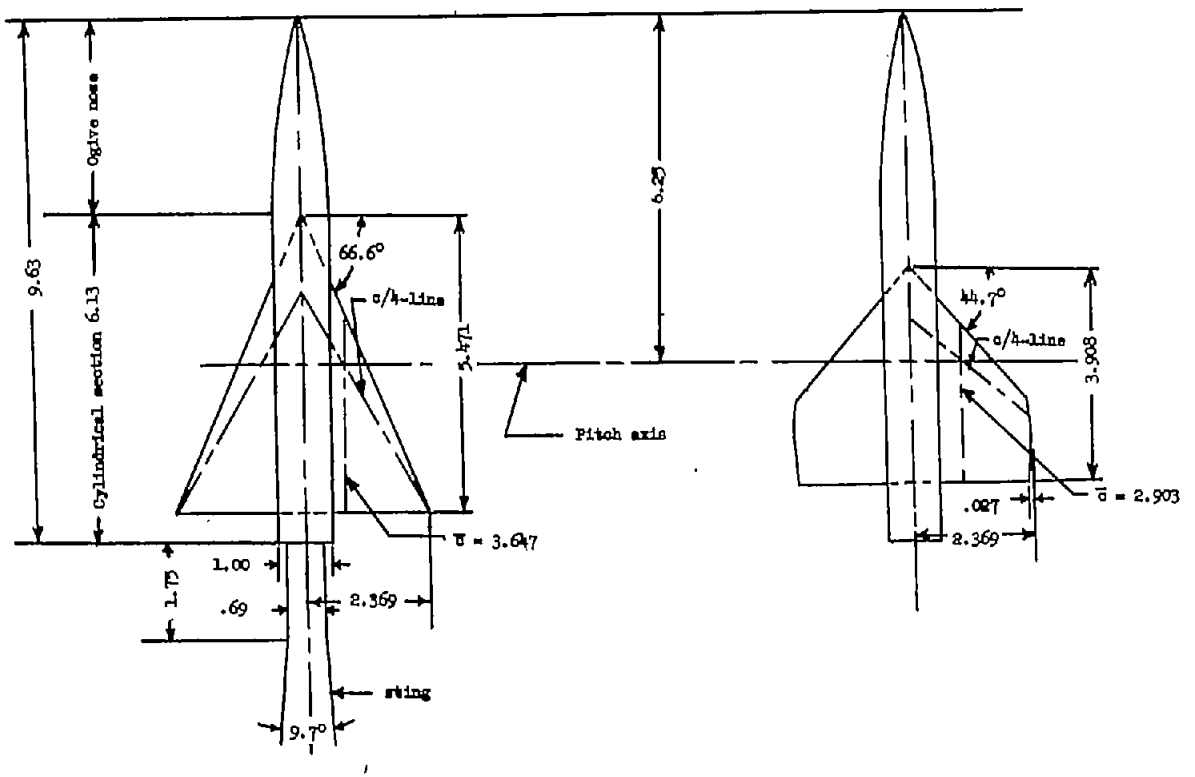

Aspect-ratio-1.73 delta-wing configuration

Aspect-ratio-1.73 clipped-wing configuration

Figure 1.- Details of the two wing-body combinations. All dimensions are in inches.

CONFIDENTIAL

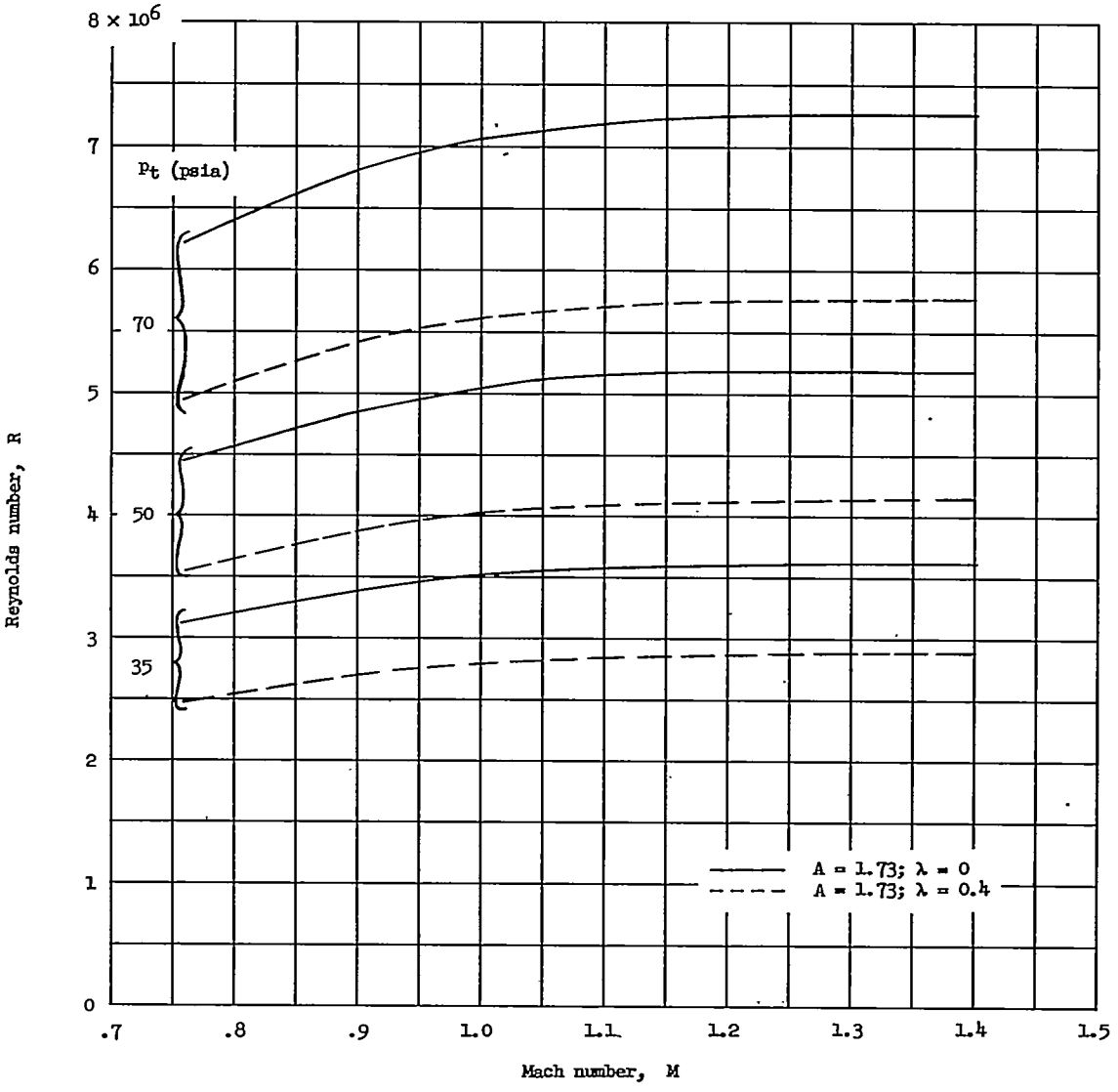

Figure 2.- Variation of Reynolds number with Mach number at various stagnation pressures for the two wing-body combinations.

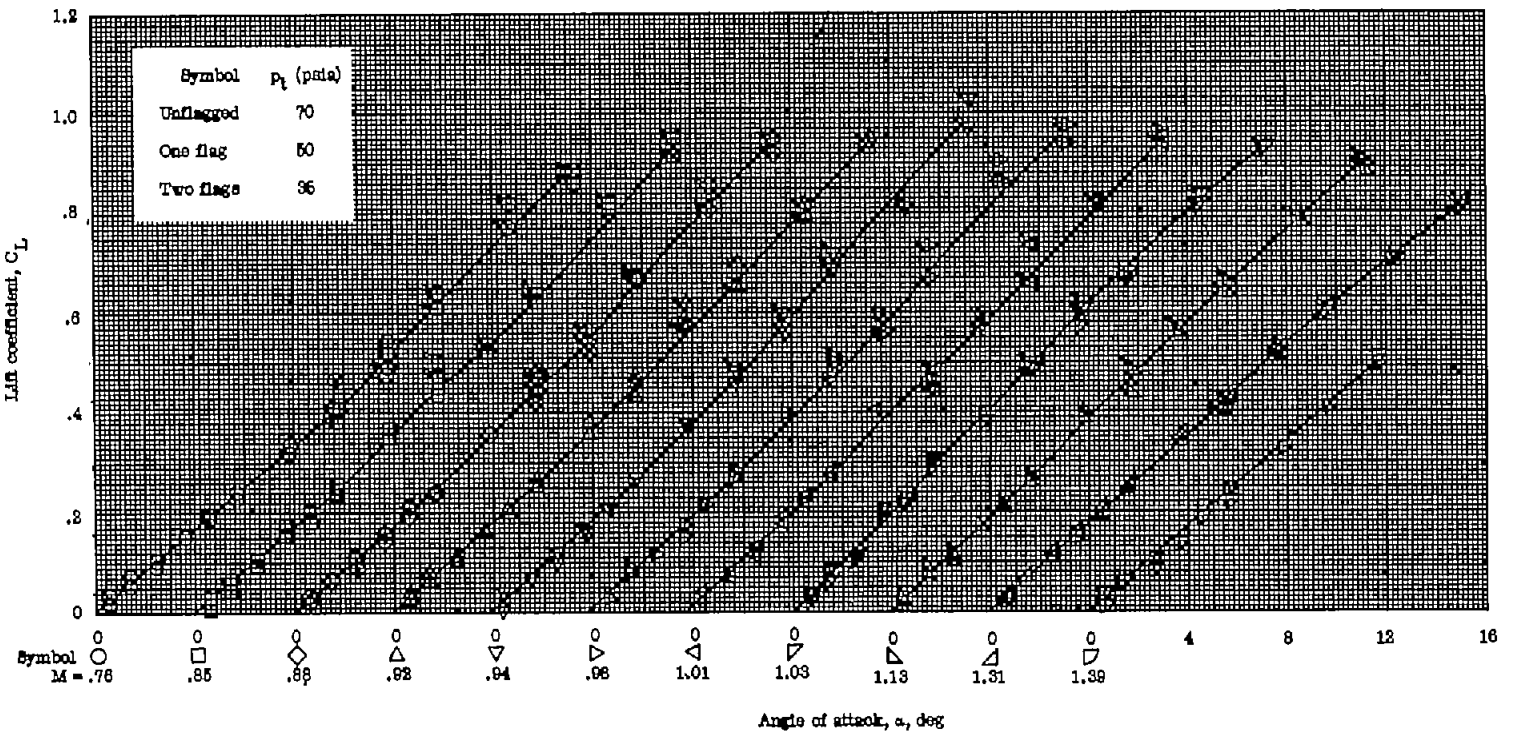

(a) $\lambda = 0$.

Figure 3.- Variation of lift coefficient with angle of attack at various Mach numbers.

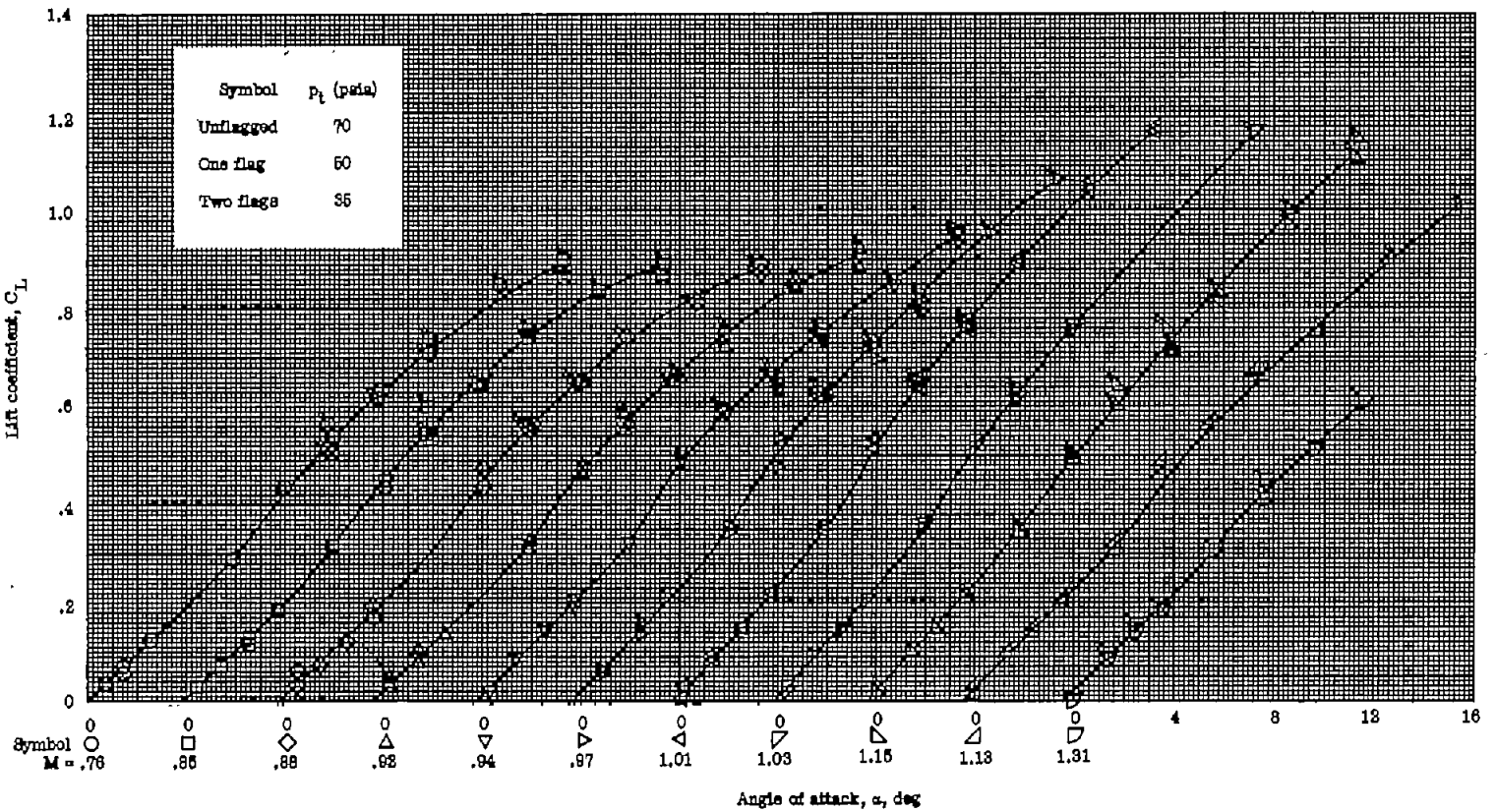

(b) $\lambda = 0.4$.

Figure 3.- Concluded.

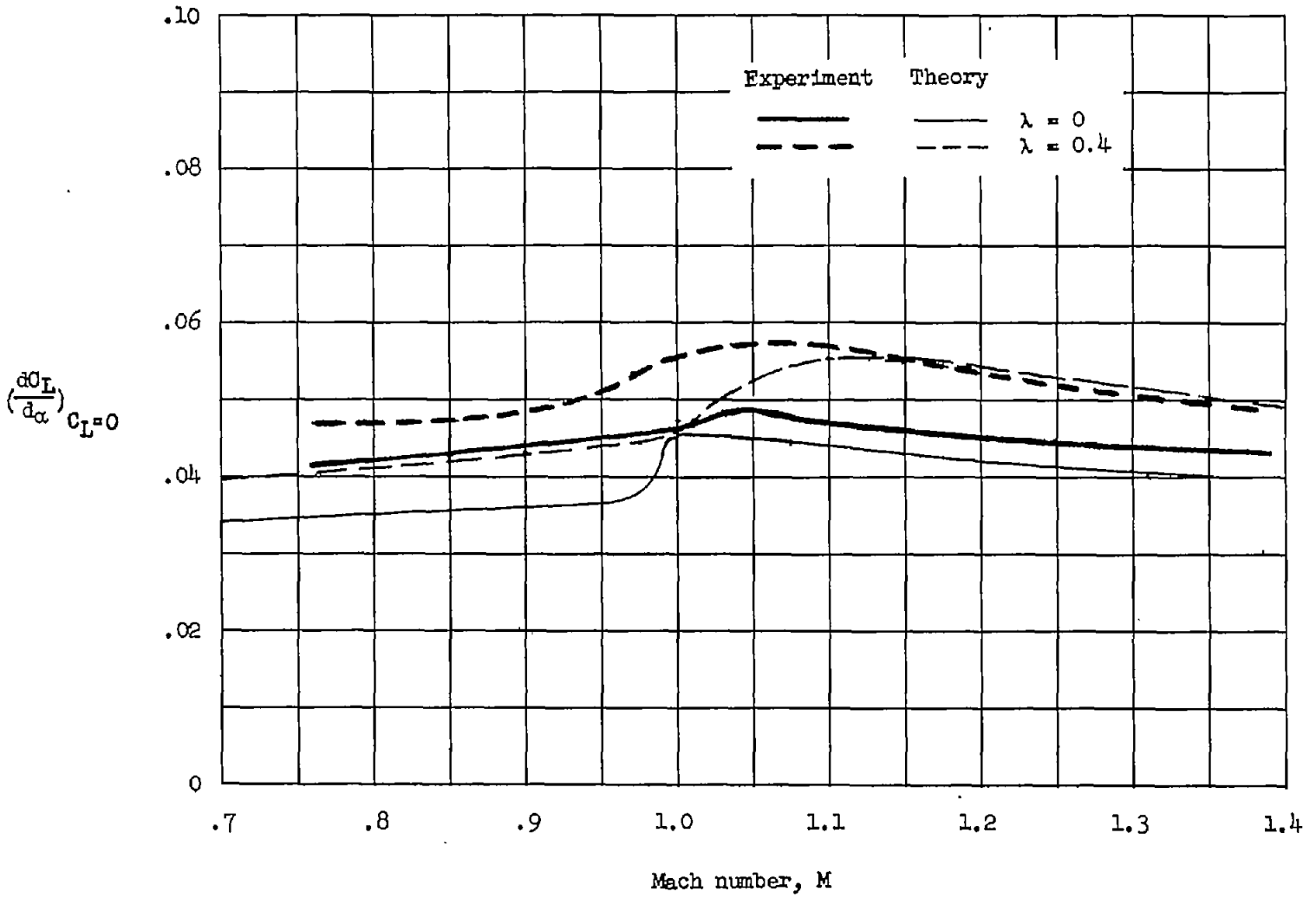

Figure 4.- Variations of lift-curve slope at zero lift with Mach numbers.

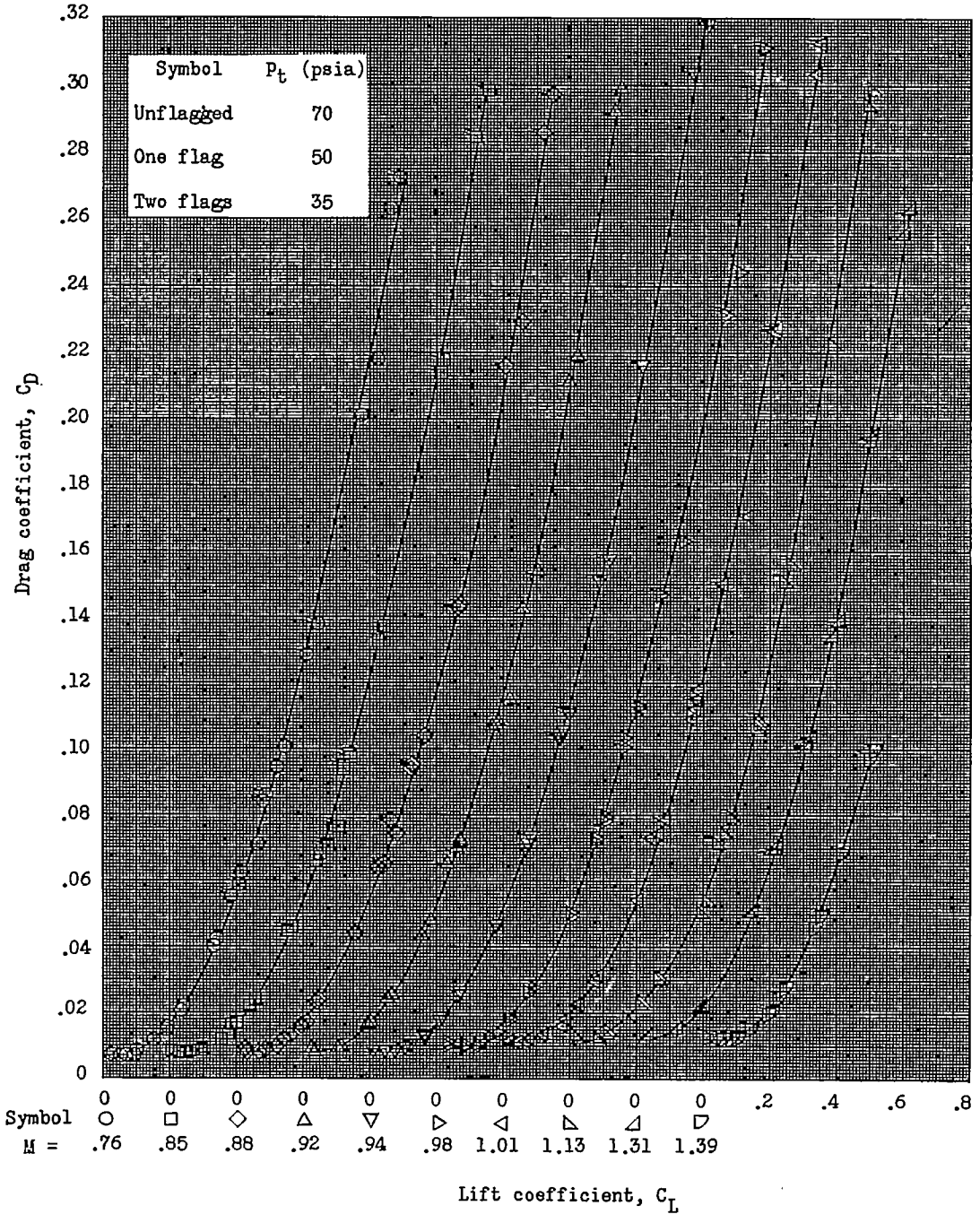

(a) $\lambda = 0$.

Figure 5.- Variation of drag coefficient with lift coefficient at various Mach numbers.

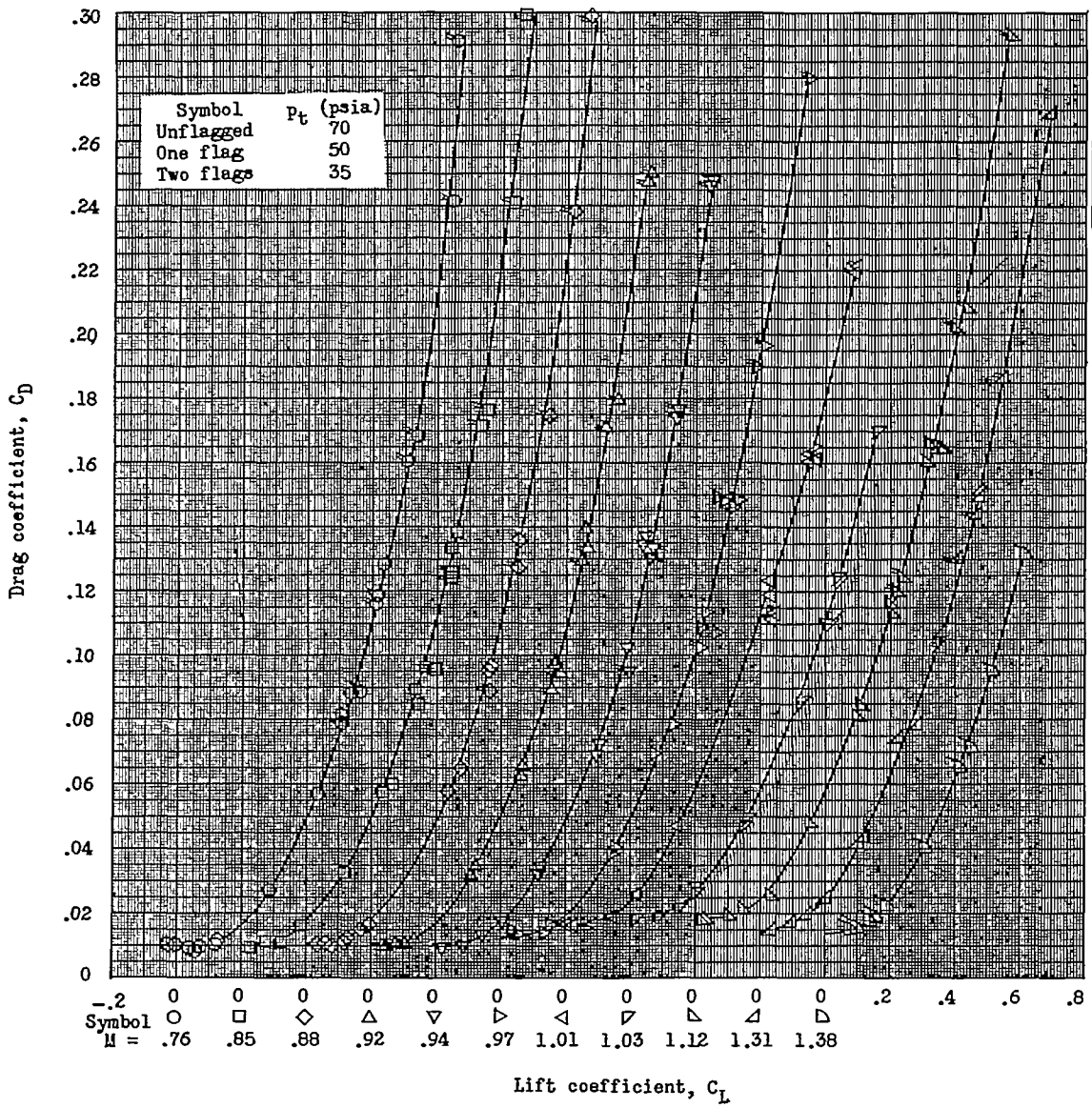

(b) $\lambda = 0.4$.

Figure 5.- Concluded.

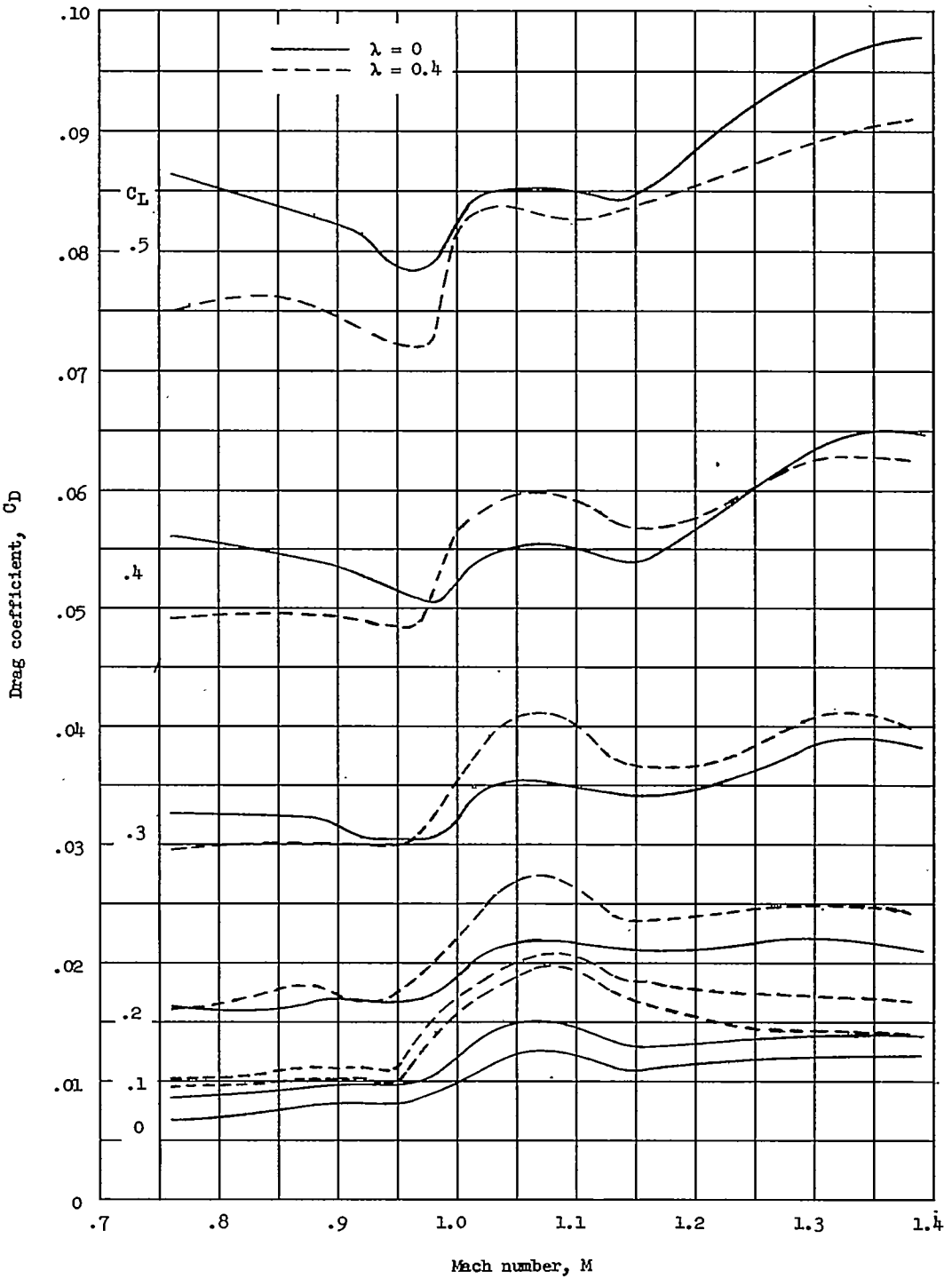

Figure 6.- Variations of drag coefficient with Mach number at various values of lift coefficient.

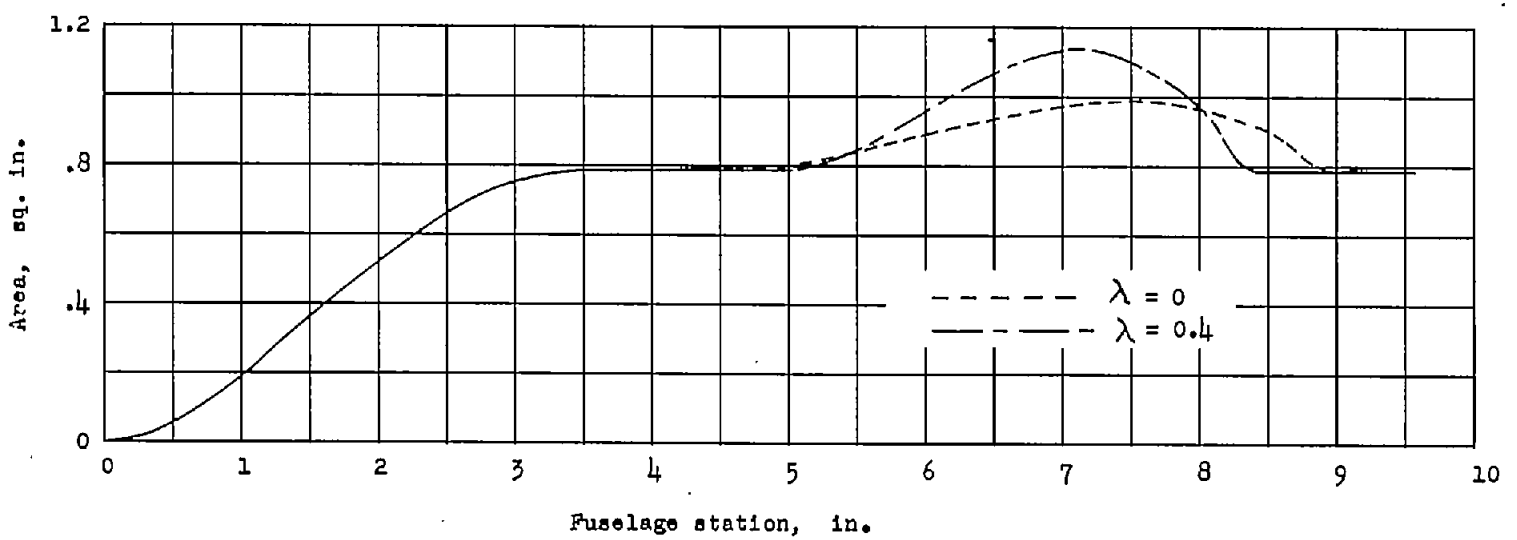

Figure 7.- Longitudinal area development of the wing-fuselage combinations at a Mach number of 1.0.

[redacted]

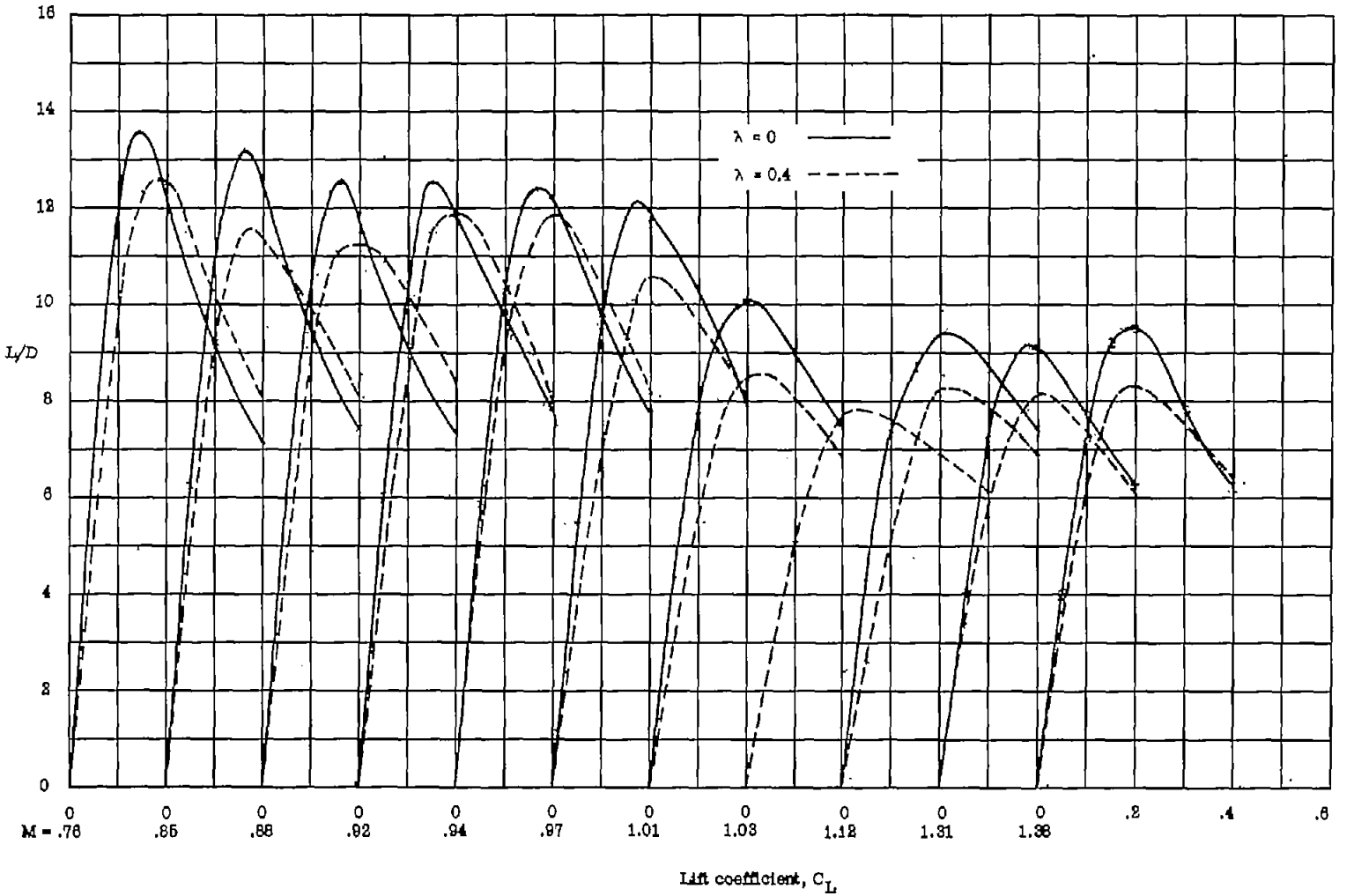

Figure 8.- Variation of lift-drag ratio with lift coefficient at various Mach numbers.

[redacted]

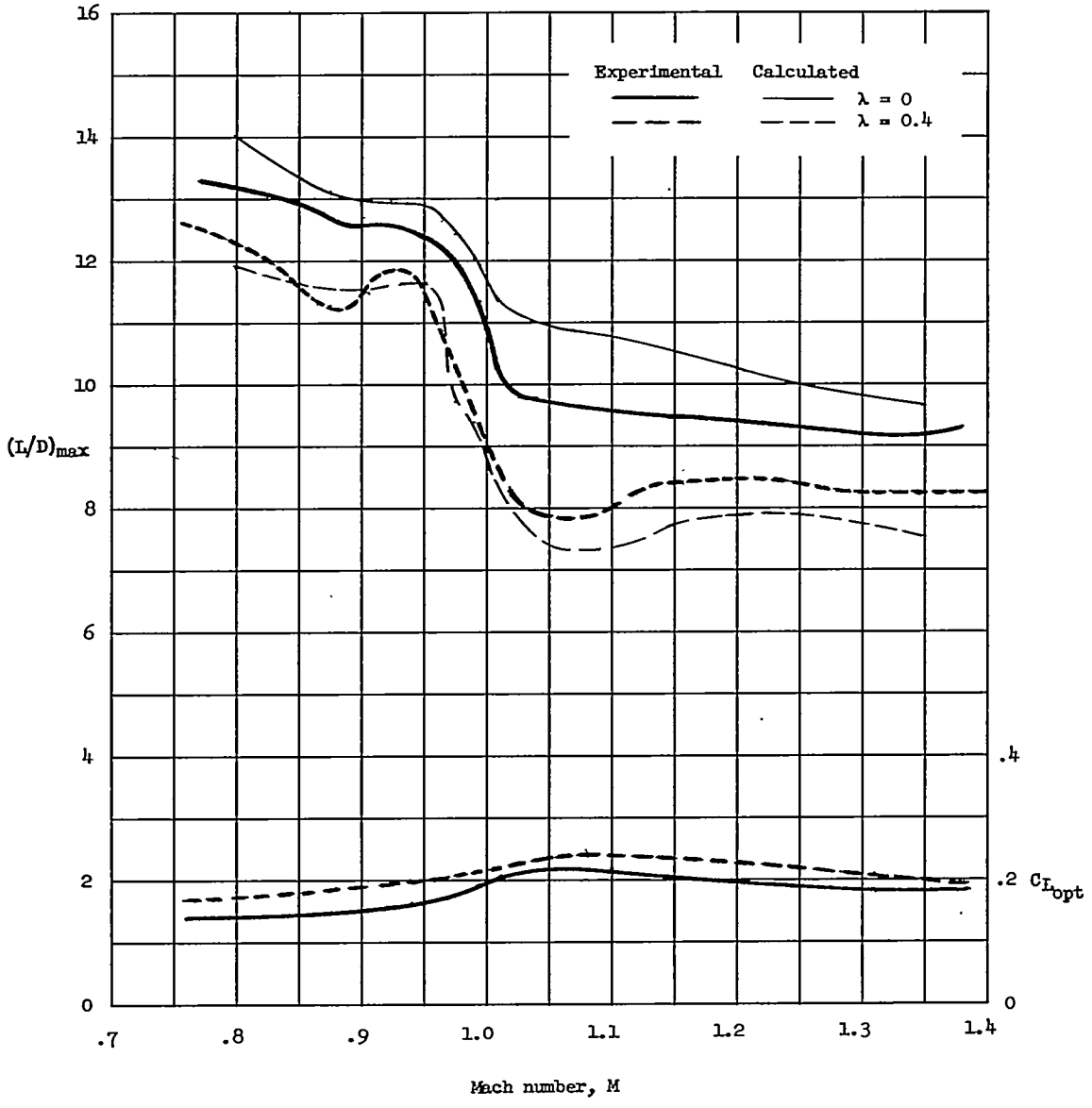

Figure 9.- Variations of $(L/D)_{max}$ and $C_{L_{opt}}$ with Mach number.

[redacted]

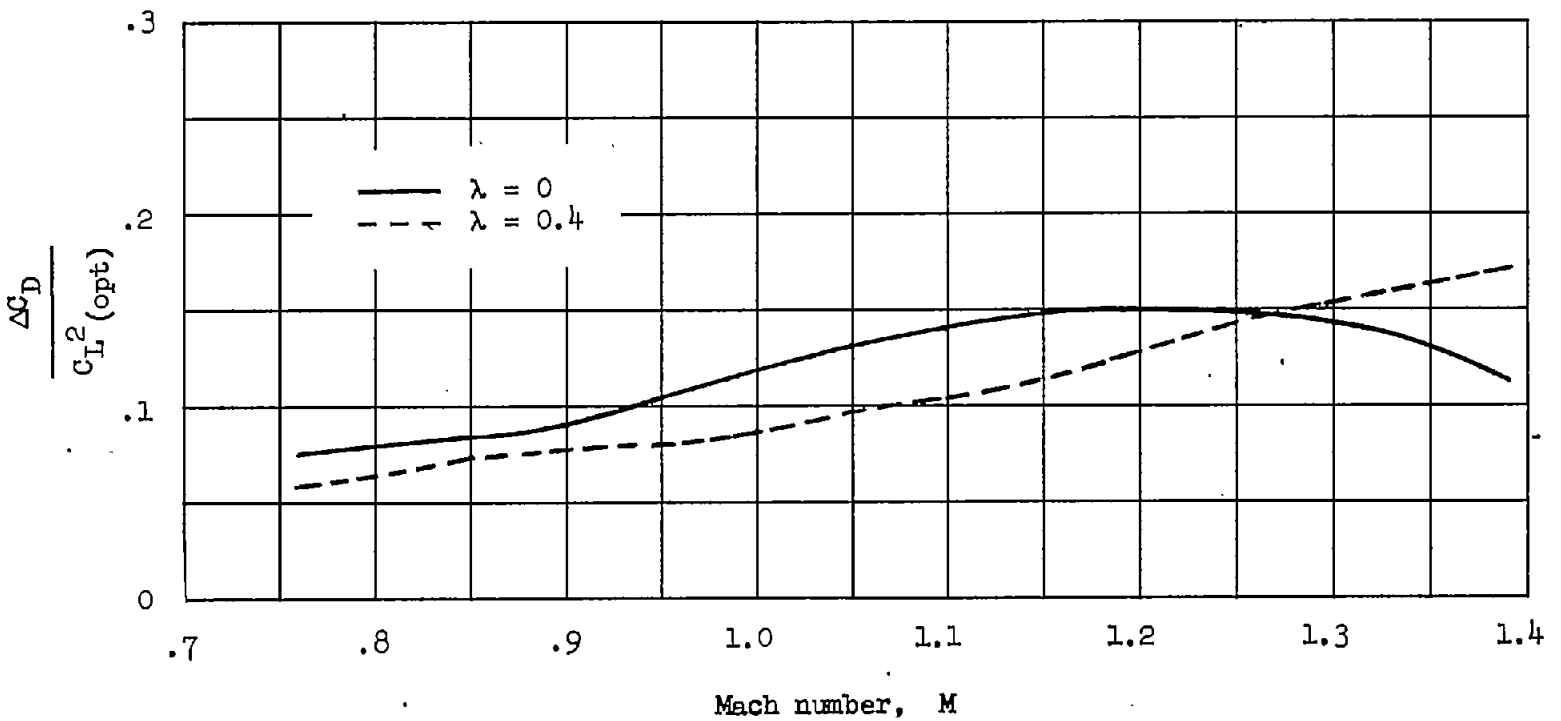

Figure 10.- Variation of drag-due-to-lift factor with Mach number at optimum lift.

[redacted]

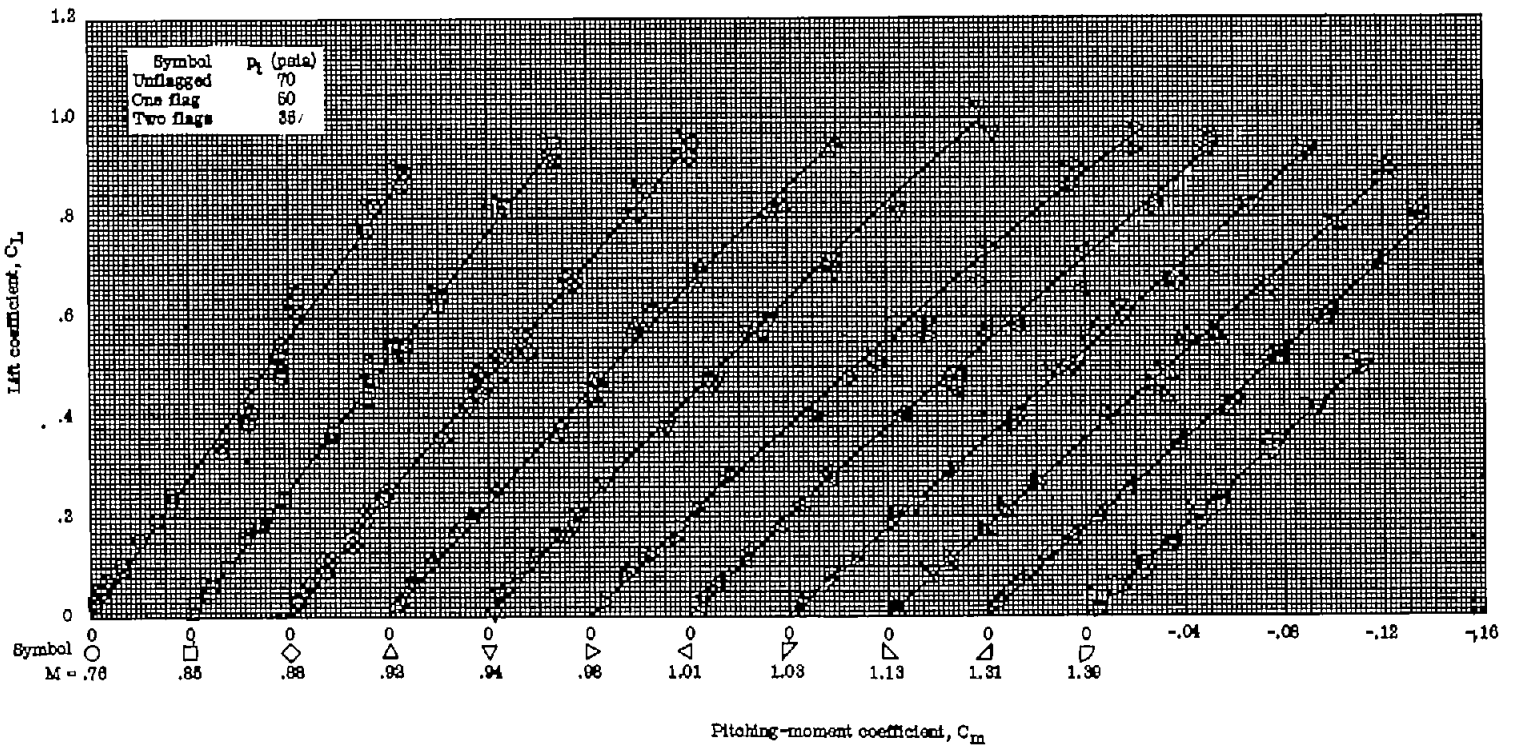

(a) $\lambda = 0$.

Figure 11.- Variation of lift coefficient with pitching-moment coefficient at various Mach numbers.

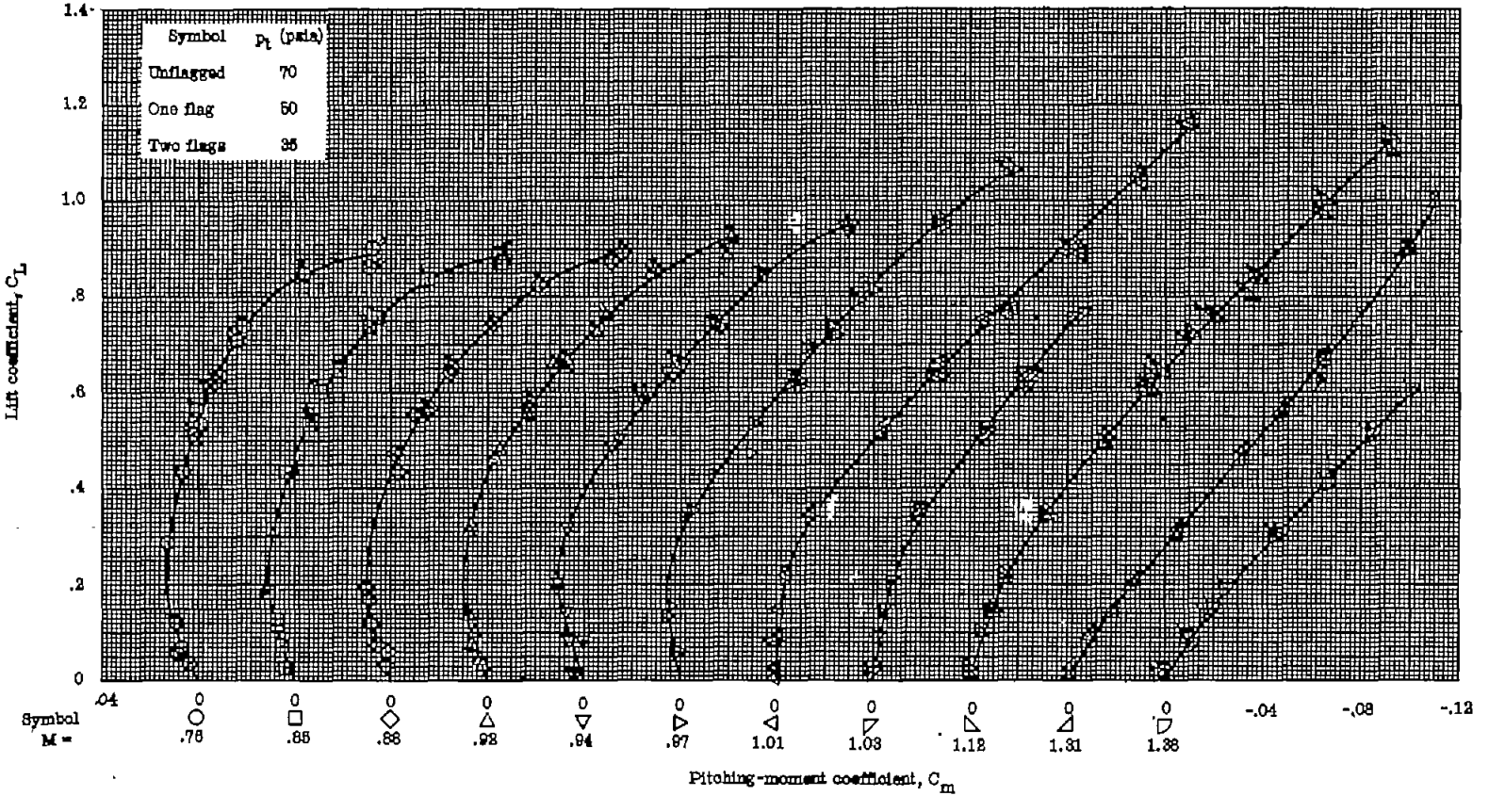

(b) $\lambda = 0.4$.

Figure 11.- Concluded.

[redacted]

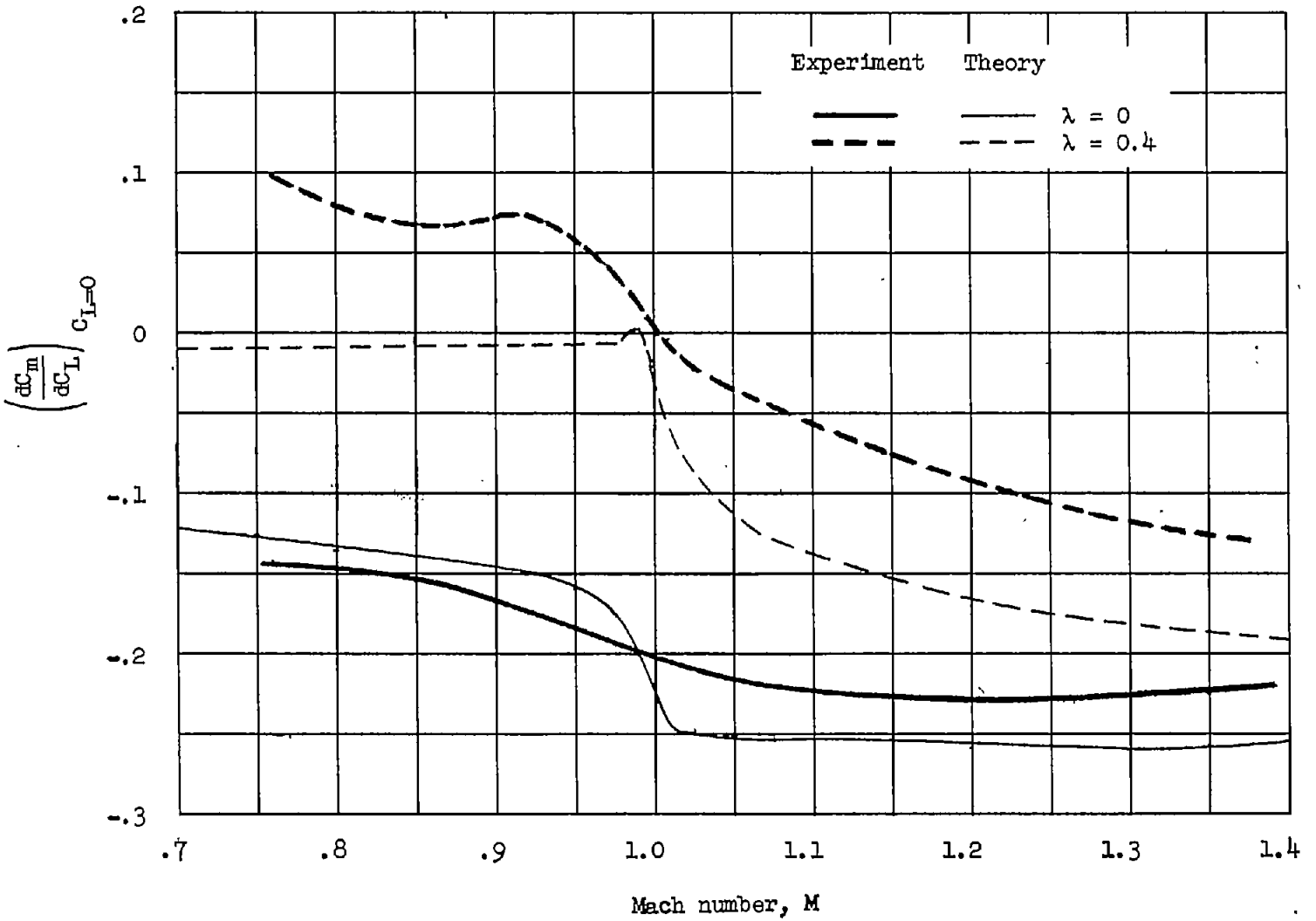

Figure 12.- Variations of slope of pitching-moment curve with Mach number.

[redacted]

[redacted]